



# Reducing the radioactive doses of liquid samples taken from reprocessing plant vessels by volume reduction

G. Janssens-Maenhout<sup>a,\*</sup>, J. Buyst<sup>b</sup>, P. Peerani<sup>a</sup>

<sup>a</sup> Institute for the Protection and the Security of the Citizen, Joint Research Centre Ispra, Via E. Fermi, 1, I-21020 ISPR, Italy

<sup>b</sup> University of Ghent, Faculty of Engineering, TW08 Technologiepark, B914, B-9052 ZWIJNAERDE, Belgium

Received 3 March 2006; accepted 26 September 2006

## Abstract

Size reduction is attractive because it should enable a solution to be analysed by much more direct, and therefore faster and simpler, methods. For instance if the traditional 7 ml vials used in reprocessing plants can be replaced by vessels containing less than 1  $\mu$ l, it should be possible to analyse the non-diluted solutions in gloveboxes. These vessels would be electro-mechanical, so the term MEMS might be appropriate.

This paper determines a conservative estimate for the dose reduction that would be obtained if microlitre samples were extracted from an input accountancy tank in a reprocessing plant, in which the spent fuel is dissolved in nitric acid. This estimate has to take into account the self-shielding effect, that varies for different low-energy and high-energy gamma-emitting isotopes. The typical composition of the solution from an input accountancy tank in a reprocessing plant is first derived by means of a burn-up code. Eight different spent fuel cases are considered to cover the range of fission products, that can emit low and high energy gamma's. The neutron and gamma fluxes emitted from the classical 7 ml vial and from a vessel with less than a microlitre solution are calculated by means of Monte Carlo simulations. The resulting doses are calculated and compared in average and in distribution for different cases of spent fuel composition. For a volume size reduction of 6300 an averaged conservative dose reduction of 6000 is obtained.

© 2006 Elsevier B.V. All rights reserved.

PACS: MCNP; SCALE; ORIGEN-S

## 1. Introduction

### 1.1. Challenges for the on-site sample characterization

In the nuclear fuel cycle, conversion, enrichment, fuel fabrication and reprocessing plants are the most vulnerable facilities from a proliferation point of view, because the nuclear material (mainly U and Pu) in these facilities is directly accessible in liquid, gas or powder form, and are therefore easier to divert than in, e.g. a reactor or in spent fuel storage. The provision of safeguards measures have been more elaborate in reprocessing and MOX fuel fabrication plants, because only these facilities deal with Pu in liquid and powder form.

In reprocessing plants there exist two methods for determining the nuclear material inventory in accountancy tanks: either by a combination of an accurate measurement of the total vol-

ume at the operating conditions and a precise sample analysis in g/l (e.g. with hybrid K-edge) or by combining the total weight of the tank inventory with an isotope dilution mass spectrometry (g/g) for sample characterisation. The first method has found more common practice, because it provides a higher throughput of samples in the analytical laboratory. As reported by Daures et al. (2003), on-site analytical laboratories have been developed to provide the fast laboratory responses that are needed for near real-time accountancy.

The sample composition is typically 3–5 M nitric acid in which per litre up to 250 g spent fuel is dissolved, leading to densities of 1.4 kg/l. Nowadays a sample of the accountancy tanks' solution is automatically sucked into a vial, that travels through a transfer line directly to the neighbouring analytical laboratory. Even with on-site laboratories, the time to report a sample analysis is affected by extensive sample preparation, for instance a pre-separation or a dilution with a factor 20,000 is needed before the sample can be analysed in a glove box. A considerable simplification in sample preparation will shorten, substantially, the measurement procedure. This simplification can be obtained

\* Corresponding author. Tel.: +39 0332 78 5831; fax: +39 0332 78 9216.  
E-mail address: [greet.maenhout@jrc.it](mailto:greet.maenhout@jrc.it) (G. Janssens-Maenhout).



Table 1  
Spent fuel models: seven variants on the reference case

Case	Enrichment (wt% U-235)	Burn-up (MWday/t)	Cooling period (days)
Reference	3.8	43,200	3650
Low enrichment	3.2	43,200	3650
High enrichment	4.2	43,200	3650
Low burn-up	3.8	36,000	3650
High burn-up	3.8	64,800	3650
Short cooling	3.8	43,200	1825
Long cooling	3.8	43,200	5475
Extreme cooling	3.8	43,200	7300

of 1 m in air, have been compared for the different spent fuel solutions that are specified in Table 1.

## 2. Set-up of the radiation source

### 2.1. Isotopic composition of the modelled spent fuel solutions

A fuel assembly with an enrichment of 3.8 wt% of U-235 and with an average power of 30 MW during three identical cycles of 480 days, corresponding to an average burn-up of 43,200 MWday/t fresh  $\text{UO}_2$  at end of life, and then allowed to cool for 10 years was selected as the reference case. Seven different variants were modelled as indicated in Table 1 to investigate the influence of the initial enrichment grade, the average burn-up and the cooling down period. With the burn-up code, SCALE, the complete fuel depletion was analysed with a 1D neutronics model for the PWR fuel, with a normalised active fuel length representing 1 t of fresh fuel<sup>2</sup>, and with decay calculations performed with the burn-up dependent cross section libraries that were contained in the ORIGEN-S module. The burn-up history was modelled by repeating a sequence of burn-up steps. The resulting isotopic compositions of each of the specified spent fuels are shown in Fig. 2.

The nuclides in the spent fuel assembly that account for a cut-off percentage of 0.05% are: U-238, contributing for over 90% to the total mass, U-235, Pu-238, Pu-239, Pu-240, Pu-241, Pu-242. In all eight cases of spent fuel the fission products contribute for almost 5% of the total mass and the actinides for a maximum 0.7%. A significant impact of increasing burn-up can be noticed by the reduction of the U-isotope and the enlarged production of fission products.

### 2.2. Neutron and gamma source for the modelled solutions

The major contributors to neutron and gamma emission were now focussed on, in order to model an appropriate neutron and gamma source for the spent fuel solution.

For the neutron source Cm-244 was found to contribute over 96% to the neutron production for all eight cases. The remaining

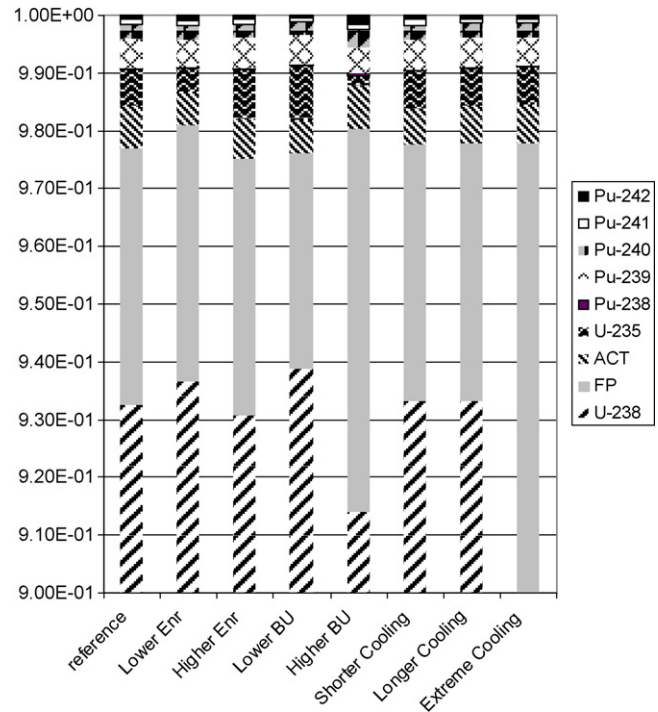


Fig. 2. Calculated isotopic composition for the eight different spent fuel cases of Table 1.

percentage of neutrons was mainly generated by  $(\alpha, n)$  reactions with Pu-238, Am-241 and Cm-244. The total spectrum of neutrons can be composed by the sum of all spontaneous fission spectra. That has been modelled within an accuracy of 2% by the spectrum of Cm-244, renormalised with the total neutrons, as shown in Fig. 3. The energy-dependence is described with the Watt-distribution formula for the Cm-244 spectrum. An extensive description is given by Buyst (2005) and full justification of the model can be found in the appendix.

For the gamma source, the fission products represent a hundred times larger source of photons than the actinides, as detailed in Table 2. The Ba-137m appears to contribute 75% to the gamma spectrum for all cases, except for the case, which had a short cooling period. In the latter case the gamma contribution of Ba-137m is limited to 50% due to the fast decay of Cs-134. The following must be summed to explain 99% of all emitted photons: Ba-137m, Ce-134, Eu-154, Sb-125 and Rh-106, and in the case of long and extreme long cooling also Am. The gamma

Table 2  
Total number of particles per second and per t spent fuel as source for MCNP

	Fission products		Actinides	
	$\gamma$ (s)	MeV (s)	$\gamma$ (s)	MeV (s)
Reference	$9.27 \times 10^{15}$	$3.15 \times 10^{15}$	$9.57 \times 10^{13}$	$2.66 \times 10^{12}$
Low enrichment	$9.10 \times 10^{15}$	$3.16 \times 10^{15}$	$1.03 \times 10^{14}$	$2.80 \times 10^{12}$
High enrichment	$9.35 \times 10^{15}$	$3.14 \times 10^{15}$	$9.16 \times 10^{13}$	$2.59 \times 10^{12}$
Low burn-up	$7.76 \times 10^{15}$	$2.56 \times 10^{15}$	$7.18 \times 10^{13}$	$2.13 \times 10^{12}$
High burn-up	$1.36 \times 10^{16}$	$4.95 \times 10^{15}$	$2.02 \times 10^{14}$	$4.43 \times 10^{12}$
Short cooling	$1.57 \times 10^{16}$	$5.67 \times 10^{15}$	$8.18 \times 10^{13}$	$2.00 \times 10^{12}$
Long cooling	$7.61 \times 10^{15}$	$2.46 \times 10^{15}$	$1.06 \times 10^{14}$	$3.17 \times 10^{12}$
Extreme cooling	$6.61 \times 10^{15}$	$2.12 \times 10^{15}$	$1.14 \times 10^{14}$	$3.55 \times 10^{12}$

<sup>2</sup> As shown by Buyst (2005) all variants could be modelled with the same active fuel length as the variation was negligible for the different cases.

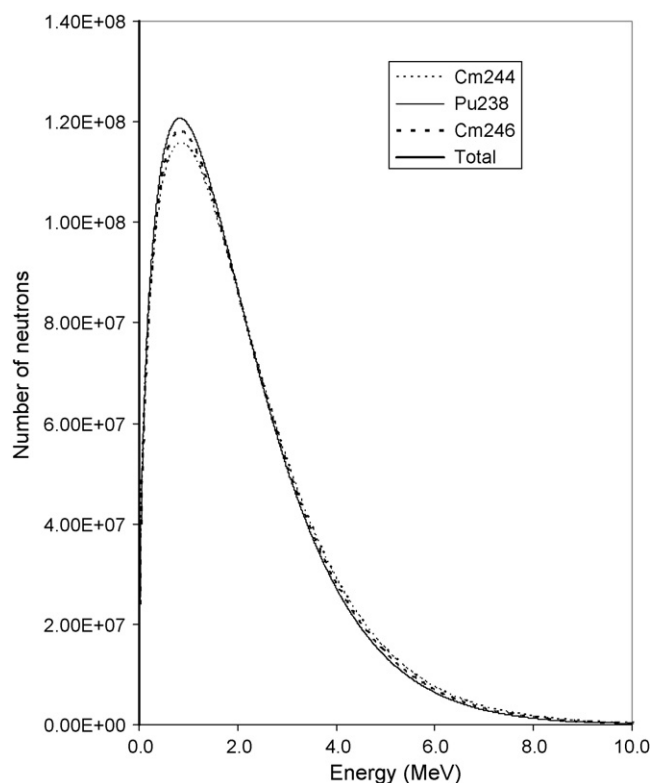


Fig. 3. Cm-244 spectrum vs. the total spectrum of the three most contributing nuclides for the reference case, that is representative for all the modelled cases of spent fuel solutions.

spectrum has been modelled within an accuracy of 0.3% by the discrete gamma spectrum composed of the spectra of the three most irradiant isotopes, that is renormalised with the total generated photons. More details on the justification of the gamma source model are extracted from Buyst (2005) and are given in the appendix.

### 3. Dose calculations

Given the fact that the sample radioactive solution is enclosed in HDPE material, the dose at contact with the HDPE, and the dose at a distance of 1 m away from the sample, should only be attributable to the neutron and gamma fluxes. The dose calculation was based on the flux-to-dose factors for neutrons and photons obtained from the 1977 ANSI/ANS and NCRP-38 databases.

The simulations were performed with the geometries as specified in Fig. 4 with materials densities of:  $1.1 \text{ g/cm}^3$  for rubber,  $0.96 \text{ g/cm}^3$  for HDPE, and  $2.65 \text{ g/cm}^3$  for quartz. The millivial contained 7 ml solution and MEMS contained  $0.636 \mu\text{l}$  solution in the analysis channel and  $0.236 \mu\text{l}$  in the inlet and in the outlet. The solution concentration was stepped from 2–25 to 100–250 g/l. The neutron and photon sources were modelled for each of the eight cases with mean values as specified in Table 3.

#### 3.1. MEMS results

The contact dose for the most conservative case, filled with 2 g/l nitric acid solution with spent fuel reaches  $7.93 \mu\text{Sv/h}$ . This

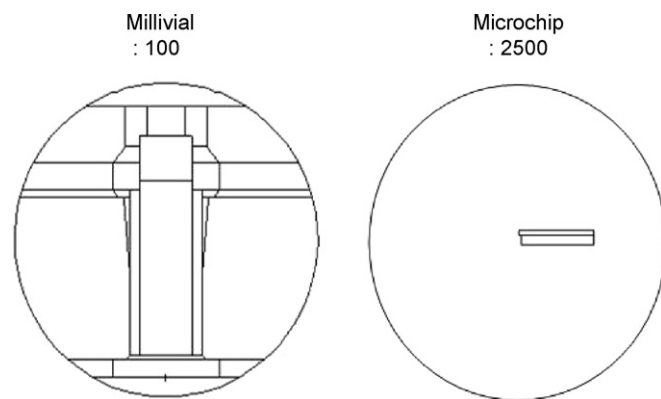


Fig. 4. Geometry applied in the MCNP calculations for the millivial (scale 1 over 1/100) and for the microchip (scale 1 over 1/25,000).

Table 3

Total number of particles per second and per t spent fuel as source for MCNP

Case	Photons ( $\gamma/\text{s/t}$ )	Neutrons ( $\text{n/s/t}$ )
Reference	$4.00 \times 10^8$	$7.24 \times 10^{15}$
Low enrichment	$5.70 \times 10^8$	$7.16 \times 10^{15}$
High enrichment	$3.21 \times 10^8$	$7.28 \times 10^{15}$
Low burn-up	$1.74 \times 10^8$	$6.01 \times 10^{15}$
High burn-up	$2.27 \times 10^8$	$10.9 \times 10^{15}$
Short cooling	$4.82 \times 10^8$	$12.6 \times 10^{15}$
Long cooling	$3.33 \times 10^8$	$5.87 \times 10^{15}$
Extreme cooling	$2.78 \times 10^8$	$5.09 \times 10^{15}$

means that a normal operator in a radiochemical facility could handle the component with a pair of gloves during the complete year, without any fear of reaching the dose limitation for hands. The very small dose at 1 m also confirms that there is no possibility of reaching the maximum effective dose limitation, for the total body, for a single year (20 mSv/year and in the near future 12 mSv/year), and for five consecutive years (100 mSv/5 year).

The gamma part represents the major contribution to the dose, because the neutron dose is a factor  $10^{-5}$  lower than the gamma dose, leading to maximum  $1.332 \mu\text{Sv/year}$ . Although the maximum dose is obtained in the case of spent fuel with short cooling, the spent fuel with high burn-up also leads to a relatively high dose. The enrichment grade characteristic shows a minor influence on the results, as shown in Table 4.

Table 4

Results of the dose caused by the gamma flux at contact and at 1 m distance for a solution of 2 g/l nitric acid with dissolved spent fuel

Case	Dose at contact ( $\mu\text{Sv/h}$ )	Dose at 1 m ( $\mu\text{Sv/h}$ )
Reference	4.57	$1.73 \times 10^{-3}$
Low enrichment	4.52	$1.71 \times 10^{-3}$
High enrichment	4.60	$1.74 \times 10^{-3}$
Low burn-up	3.80	$1.44 \times 10^{-3}$
High burn-up	6.87	$2.60 \times 10^{-3}$
Short cooling	7.93	$3.01 \times 10^{-3}$
Long cooling	3.71	$1.41 \times 10^{-3}$
Extreme cooling	3.22	$1.22 \times 10^{-3}$

For each of the eight cases of spent fuel, MCNP calculations have been performed twice, with the neutron group spectrum and with a continuous spectrum.

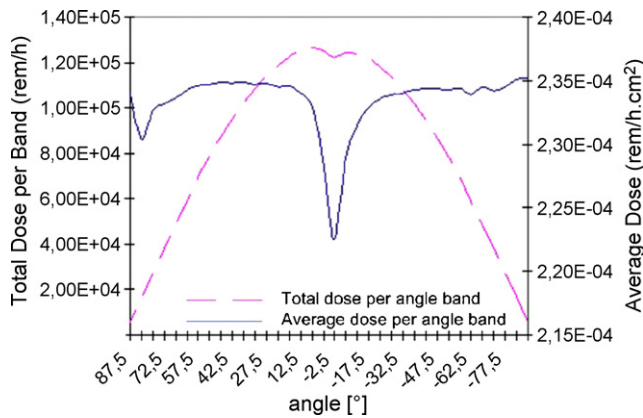


Fig. 5. Distribution of the dose from +90° above the mid plane to −90° below the mid plane of the microchip (reference case with 2 g/l solution).

The dose calculations have been performed with a six-group spectrum for the neutron part, and a discrete spectrum for the gamma part. It was observed that the neutron dose calculations with the continuous spectrum yields an up to 20% lower dose than those with the group spectrum, which justifies the use of the group spectrum. In contrast, the calculations with the group spectrum and with the discrete spectrum for the gamma dose have shown a difference of less than 1%. This justifies the use of a renormalised Ba-137m discrete spectrum. More details are given in Tables A1 and A2 of the appendix.

Given the flat geometry of the MEMS, a non-uniform distribution of the dose is expected, which is governed by the photon dose. Fig. 5 shows the angular dependency of the dose, which clearly shows that the particles emitted in the plane of the microchip (at the angle around 0°) lead to the lowest dose contribution, because the particles have to penetrate at least 1 mm of thermalising material. Under an angle substantially different from 0°, the particles can profit from a faster exit out of the thermalising material, up to 0.3 mm for the upwards directed ones and up to 0.5 mm for the downwards directed ones.

Two simplified models, that could be easily used in optimisation studies, were evaluated: a point source and a line source with the same intensity. For the neutron dose the simplified line source gives a very small overestimation of only 0.69% and the point source overestimates by only 0.65%. For the gamma dose the simplification in geometry has a larger impact, the simplified line source gives an overestimation of 2.73% and the point source overestimates by 2.90%.

### 3.2. Dose reduction versus volume reduction

It has been shown above that the absolute dose at contact should be well below all official dose limitations. Here the minimum percentage of dose reduction obtained by reducing volume size is discussed. To derive the relative dose reduction obtained by volume reduction, the doses emitted at a distance of 1 m are compared for both the millivial and the proposed device.

Table 5

The reduction of the dose at 1 m distance for the microchip relative to the millivial has been calculated in function of different common solution concentrations

Concentration U-Pu (g/l)	U-Pu mass (μg)	Mass reduction	$R_D$ at 1 m
2	2	7000	6092
25	28	6250	6046
100	111	6306	5958
250	221	6335	5896

The dose reduction factor has been averaged over all eight spent fuel cases.

The volumetric reductions can be accurately calculated by taking into account the actual geometries of both components, assuming that the millivial is systematically filled with 7 ml solution and that there are no gas bubbles when the MEMS is completely filled. The volume of the proposed device is 6321.07 times smaller than the millivial. Given the fact that nowadays, with high burn-up fuel, either a pre-separation or a dilution factor of 20,000 is needed before the sample solution can be analysed, it is obvious that future geometries will be downscaled by this order of magnitude. A further factor of three is feasible with regard to manufacturing, but would require higher electrical forces to fill the micro channel.

To determine the gain in dose reduction for the most conservative case, a dose reduction factor  $R_D$  has been defined as the ratio of the lowest dose for the millivial  $D_m$  to the highest dose of the MEMS  $D_\mu$  caused by neutrons  $n$  and photons  $\gamma$  calculated either with the group spectrum (index  $g$ ), or with the renormalised continuous Watt spectrum of Cm-244 neutrons and the renormalised discrete photon-spectrum of Ba-137m (index  $c$ ), more specifically by

$$R_D = \frac{\min(D_m^{n,g}, D_m^{n,c}) + \min(D_\mu^{\gamma,g}, D_\mu^{\gamma,c})}{\max(D_\mu^{n,g}, D_\mu^{n,c}) + \max(D_\mu^{\gamma,g}, D_\mu^{\gamma,c})}$$

The results are for a solution of 2 g/l dissolved spent fuel 6092, meaning that 96.4% of proportional dose reduction with volume size reduction is achieved. No differences larger than 0.1% could be observed in the results for the eight cases of specified spent fuel. Similar calculations of dose reduction have been carried out for other concentrations and have to be compared with the volume reduction of 6321. The resulting characteristics (in mass content) with dose reduction and mass reduction for the different types of solutions are given in Table 5. Even at highly concentrated solutions a dose reduction of 5896 for the given volume size reduction is obtained. It can be concluded that for solutions with up to 250 g/l dissolved spent fuel, even of high burn-up and short cooling time a minimum percentage of 93.27 of dose reduction with the volume size reduction is guaranteed.

## 4. Conclusion

A specific MEMS for analyzing radioactive solutions of an input solution (with concentrations varying from 2 till 250 g/l) has been designed with three microchannels of 300 μm × 300 μm cross section and 18 mm length. One channel contains the reference solution with neodymium, the channel in the centre is the blank and the third channel contains the

sample. The concentration of the solution is determined by the photospectra of the light transmitted along the channel axis and absorbed at nuclide-specific wavelengths.

The dose reduction by volume size reduction has been determined by Monte Carlo simulations. If the volume of a typical input solution sample is reduced with a factor 6321 (for the proposed MEMS design) a dose-reduction of 5896 is achieved for the highly concentrated solution of 250 g/l. The dose reduction is almost proportional with the size reduction for the different types of fuel (UO<sub>2</sub> and MOX) and for a burn-up varying from 36,000 to 64,800 MWday/t, which confirms that the change in self-shielding for the low energy  $\gamma$ -rays is very small.

### Appendix A. The microchip dose calculations with MCNP

#### A.1. Model of neutron and gamma source

In order to create an efficient time-dependent neutron source model for the Monte Carlo simulations, it was investigated if the sum of all spontaneous fission spectra cannot be replaced by the spectrum of the most contributing nuclide Cm-244. As shown in Fig. 3 the Cm-244 spectrum did not differ more than 2% from the cumulative spectrum of the three most contributing nuclides (Cm-244, Pu-238 and Cm-246). This justified to take the Cm-244 spectrum, renormalised with the total neutrons (generated by spontaneous fission and by  $(\alpha, n)$  reactions) as input to model the neutron source for the input accountancy solution. In addition Fig. A1 shows that the theoretical decay of Cm-244 in a cooling period of minimum 900 days corresponds to the decrease in neutron generation that was calculated with SCALE.

Concerning the energy-dependence of the neutron source model, the application of the continuous Watt-distribution spectrum of Cm-244 was evaluated. In order to guarantee that the continuous Cm-244 spectrum gives a conservative estimation of the neutron source, it is needed to compare the calculated group spectrum with the theoretical group spectrum, derived by integrating the continuous spectrum over the energy intervals as defined for the SCALE simulations. Fig. A2 shows that the sec-

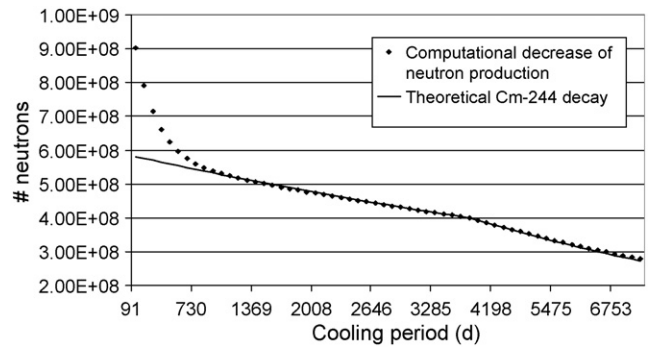


Fig. A1. The simulated neutron generation decreases with time compared to the theoretical decay of Cm-244.

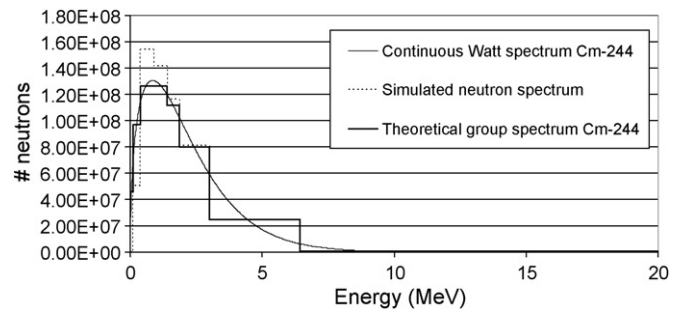


Fig. A2. Neutron spectrum as input: continuous Watt spectrum and simulated group spectrum.

ond and third energy group are not modelled in a conservative way by the theoretical spectrum. Neutrons have been neglected in the lower energy range and substituted by neutrons in the higher energy range in the SCALE calculations. Therefore both cases, the simulated group spectrum and the continuous spectrum have been taken into account for the MCNP calculations.

The gamma group spectrum resulting from the SCALE simulations has been compared to a discrete gamma spectrum composed of the spectra of Ba-137m, Cs-137 and Eu-154, that is renormalised with the total generated photons. The comparison in Fig. A3 allows to create an efficient gamma source model, by replacing the gamma group spectrum with the composed discrete spectrum.

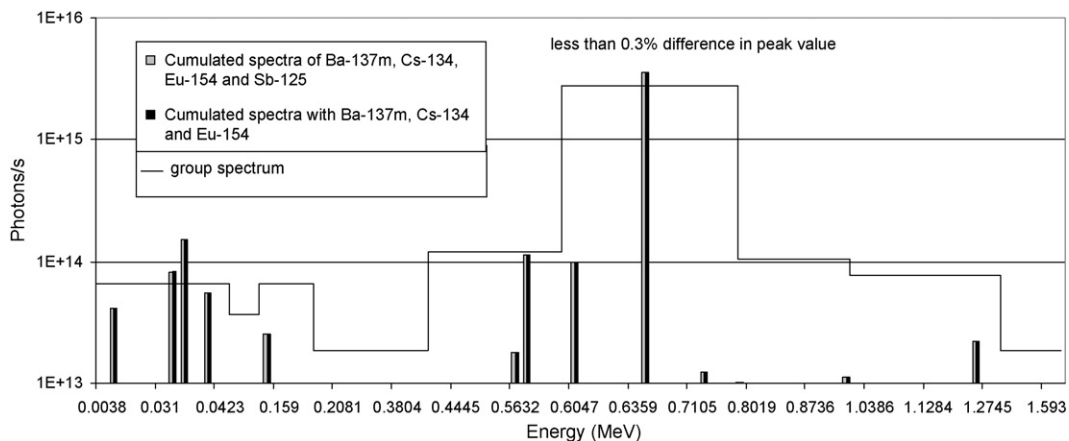


Fig. A3. Comparison of discrete gamma spectra with the three major contributing isotopes and with the four major contributing isotopes, as well as the gamma group spectrum, for the representative reference case.

Table A1

Results of the dose caused by the neutron flux at contact and at 1 m distance for a solution of 2 g/l nitric acid with dissolved spent fuel

Case	Dose at contact ( $\mu\text{Sv/h}$ )		Dose at 1 m ( $\mu\text{Sv/h}$ )	
	By group spectrum	By continuous spectrum	By group spectrum	By continuous spectrum
Reference	$2.68 \times 10^{-5}$	$2.23 \times 10^{-5}$	$1.02 \times 10^{-8}$	$8.52 \times 10^{-9}$
Low enrichment	$3.82 \times 10^{-5}$	$3.18 \times 10^{-5}$	$1.46 \times 10^{-8}$	$1.21 \times 10^{-8}$
High enrichment	$2.15 \times 10^{-5}$	$1.79 \times 10^{-5}$	$8.20 \times 10^{-9}$	$6.83 \times 10^{-9}$
Low burn-up	$1.16 \times 10^{-5}$	$9.69 \times 10^{-6}$	$4.44 \times 10^{-9}$	$3.70 \times 10^{-9}$
High burn-up	$1.52 \times 10^{-4}$	$1.26 \times 10^{-4}$	$5.79 \times 10^{-8}$	$4.82 \times 10^{-8}$
Short cooling	$3.23 \times 10^{-5}$	$2.69 \times 10^{-5}$	$1.23 \times 10^{-8}$	$1.03 \times 10^{-8}$
Long cooling	$2.23 \times 10^{-5}$	$1.86 \times 10^{-5}$	$8.51 \times 10^{-9}$	$7.09 \times 10^{-9}$
Extreme cooling	$1.86 \times 10^{-5}$	$1.55 \times 10^{-5}$	$7.10 \times 10^{-9}$	$5.91 \times 10^{-9}$

For each of the eight cases of spent fuel, MCNP calculations have been performed twice, with the neutron group spectrum and with a continuous spectrum.

Table A2

Results of the dose caused by the gamma flux at contact and at 1 m distance for a solution of 2 g/l nitric acid with dissolved spent fuel

Case	Dose at contact ( $\mu\text{Sv/h}$ )		Dose at 1 m ( $\mu\text{Sv/h}$ )	
	By group spectrum	By discrete spectrum	By group spectrum	By discrete spectrum
Reference	4.59	4.57	$1.74 \times 10^{-3}$	$1.73 \times 10^{-3}$
Low enrichment	4.56	4.52	$1.73 \times 10^{-3}$	$1.71 \times 10^{-3}$
High enrichment	4.60	4.60	$1.74 \times 10^{-3}$	$1.74 \times 10^{-3}$
Low burn-up	3.79	3.80	$1.43 \times 10^{-3}$	$1.44 \times 10^{-3}$
High burn-up	6.90	6.87	$2.61 \times 10^{-3}$	$2.60 \times 10^{-3}$
Short cooling	7.96	7.93	$3.02 \times 10^{-3}$	$3.01 \times 10^{-3}$
Long cooling	3.69	3.71	$1.40 \times 10^{-3}$	$1.41 \times 10^{-3}$
Extreme cooling	3.19	3.22	$1.20 \times 10^{-3}$	$1.22 \times 10^{-3}$

For each of the eight cases of spent fuel, MCNP calculations have been performed twice, with the neutron group spectrum and with a continuous spectrum.

## A.2. Results for neutron and gamma source separately

The dose for the microchip, filled with a solution of 2 g/l dissolved spent fuel, that is caused by the neutrons and by the gamma's has been calculated separately for the neutrons and the gamma's and in two different ways, by applying a group spectrum or a continuous spectrum for the neutrons and by a group spectrum or a discrete spectrum for the gamma's. The results are shown in the Tables A1 and A2 below.

## References

- Buyst, J. 2005. Nuclear safeguards by lab on the microchip: deterministic calculation of radioactive dose reduction by volume size reduction, Technical Report master thesis for the degree of engineering in physics, University Ghent, Fac. of engineering.
- Daires, P., Richir, P., Cremer, B., Ottmar, H., Mayer, K., Blohm-Hieber, U., Decobert, G., Rincel, X., 2003. Commissioning and routine operation of the "laboratoire sur site". In: Proceedings of ESARDA Symposium (Brugge).
- Gad-el Hak, M., 1999. The fluid mechanics of microdevices—the freeman scholar lecture. ASME J. Fluids Eng. 121, 5.
- Lascola, R.J., Livingston, R.R., Sanders, M.A., McCarty, J.E., Cooper, G.A., 2002. On Line Spectrophotometric Measurement of Uranium and Nitrate in h Canyon, Technical Report WSRC-TR-2002-00334 (rev. 0). West-inghouse Savannah River Company.
- Macerata, E. 2004. Micro-fluiddynamic constraints for the lab on the microchip to analyse radioactive solutions, Technical Report master thesis for the degree of nuclear engineering, Polytechnic of Milan, Nucl. Eng. Dep.
- Matthews, R. M. 2005. Thermo-fluid-dynamic evaluation of a micro-electromechanical device for the analysis of radioactive solutions, Technical Report thesis for the degree of engineering, University Glasgow, Mech. Eng. Dep.
- Nucifora, S. 2004. Nuclear safeguards by lab on the microchip: spectrophotometric tests of radioactive solution on microsample, Technical Report master thesis for the degree of nuclear engineering, Polytechnic of Milan, Nucl. Eng. Dep.
- Uyttenhove, W. 2005. Thermodynamic evaluation of a microchip to analyse radioactive solutions, Technical Report master thesis for the degree of nuclear engineering, University Ghent, BNEN specialisation.